Pure & Appl. Chem., Vol. 59, No. 2, pp. 161–172, 1987.
Printed in Great Britain.

Use of high pressure kinetic studies in determining inorganic substitution mechanisms

André E. Merbach

Institut de chimie minérale et analytique, Université de Lausanne, 3, Place du Château, CH-1005 Lausanne, Switzerland

Abstract - High pressure kinetic studies are particularly useful for the determination of the activation mode of simple inorganic substitution processes. Applications to solvent exchange and complex formation reactions of tetrahedral and octahedral species in aqueous and non-aqueous solvents are presented. The gradual substitution mechanism changeover revealed by variable pressure studies for both di- and trivalent hexasolvates along the first row transition metal ions is discussed. Some methodological and technical aspects of high pressure high resolution multinuclear magnetic resonance applied to solvent exchange studies are treated.

INTRODUCTION

The usual approach to elucidate the mechanisms of substitution reaction involves the study of the dependence of the reaction rate on reactants concentration, pH, ionic strength, temperature and solvent composition. The deduced empirical rate law, the electronic and steric effects induced by variations of leaving, entering, and non-reacting ligands on the rate constant, and all the available experimental and theoretical chemical information collected on the investigated reaction are then used to assign a mechanism. Even so, additional experiments may be needed to further strengthen the assignment or to distinguish between alternatives.

Pressure is one of the fundamental physical variables influencing the rate of a substitution reaction in solution and is widely used to supplement mechanistic assignment (ref. 1). However, even if the first high pressure kinetic study in coordination chemistry is almost thirty years old (ref. 2), it is only during the last decade that a tremendous activity in this field has developed. This is related to the adaptation of most fast reaction techniques for use in high pressure kinetics : stopped-flow, temperature jump, pressure jump, and nuclear magnetic resonance (ref. 3).

In the present lecture, I will try to answer the title question with the help of chosen examples, and will focus on solvent exchange and complex formation reactions of tetrahedral and octahedral species. But I will first discuss some methodological and technical aspects of these studies.

ACTIVATION VOLUME

In the transition state theory, the volume of activation $\Delta V^{\#}$, the difference between the partial molar volumes of the transition state and the reactants, is related to the pressure derivative of lnk by Eqn.1. $\Delta V^{\#}$ may be positive or negative, depending if the reaction

$$(\partial \ln k/\partial P)_T = - \Delta V^{\#}/RT \qquad (1)$$

is slowed down or accelerated with pressure. Various mathematical descriptions have been proposed to account for the pressure dependence of $\Delta V^{\#}$. The most popular is the quadratic Eqn.2, where $\Delta V^{\#}$ is the volume of activation at zero pressure and $\Delta \beta^{\#}$ is the compressi-

$$\ln k = \ln k_0 - \Delta V^{\#}P/RT + \Delta \beta^{\#}P^2/2RT \qquad (2)$$

bility coefficient of activation, a measure of the pressure dependence of $\Delta V^{\#}$.

Bond stretching in a simple dissociative step gives rise to an increase in volume, which is manifested in a decrease in the rate of reaction with increasing pressure, i.e. a positive $\Delta V^{\#}$. Conversely, bond formation occurring in a simple associative process will lead to an increase in the rate constant with increasing pressure, i.e. a negative $\Delta V^{\#}$. For substi-

tution reactions, the changes in solvent electrostriction when ions or dipoles are formed or neutralized at the transition state represents another important contribution to $\Delta V^{\#}$. The measured volume of activation $\Delta V^{\#}$ is therefore usually considered to be the combination of an intrinsic contribution $\Delta V^{\#}_{int}$, resulting from changes in internuclear distances within the reactants during the formation of the transition state, and from an electrostrictive contribution $\Delta V^{\#}_{elec}$. Unfortunately, for substitution reactions involving charged species, the observed $\Delta V^{\#}$ may be dominated by the effect of electrostriction $\Delta V^{\#}_{elec}$, to the extent that the sign of $\Delta V^{\#}$ may even differ from that of $\Delta V^{\#}_{int}$.

For solvent exchange the interpretation of $\Delta V^{\#}$ is fortunately simplified, due to the absence of electrostrictive changes (i.e. $\Delta V^{\#} \simeq \Delta V^{\#}_{int}$). Therefore, the sign of $\Delta V^{\#}$ is immediately a diagnostic of the activation step : positive for bond stretching or negative for bond making (ref. 1).

METHODOLOGY

A clear understanding of the dynamics of the solvated metal ion is essential for the correct understanding of the more complicated metal complexes. Some problems are, however, hidden behind the apparent simplicity of the perfectly symmetrical solvent exchange reaction (Eqn. 3). Reactants and products are identical and it is impossible to change their

$$MS_n^{z+} + n^*S \underset{}{\overset{k_{ex}}{\rightleftharpoons}} M^*S_n^{z+} + nS \qquad (3)$$

concentration without the use of mixed solvents, an unadvisable practice sometimes leading to controversial interpretation of results. Nevertheless, one is sometimes forced to have recourse to inert diluents, which, although not participating in the exchange reaction, form the bulk of the solution.

First order rate constants for solvent exchange are spread over a wide scale. In water at 298 K, for instance, as can be seen in Fig. 1, they range from 10^{-8} s^{-1} for Rh^{3+} to little less than 10^{10} s^{-1}. For slow reactions ($t_{1/2}$ > 0.1 s), the depletion or enrichment of a marked exchanging solvent molecule in a specific isotope can be followed by NMR or mass spectrometry. For faster exchanges, NMR line-broadening is the dedicated technique which has allowed the study of reactions with $t_{1/2}$ as short as 10^{-9} s (ref. 4) for paramagnetic systems, and it has been used for many years in kinetic studies in solution (ref. 5).

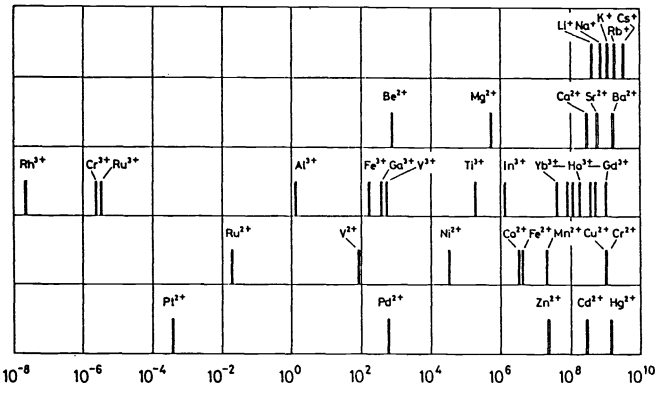

Fig. 1. Rate constants for water exchange on metal cations measured by NMR (solid bars), except for Cr^{3+}, or derived from complex formation reactions data from ref. 6 (open bars).

Fig. 2 shows the effect of pressure on ^1H-NMR spectra for tetramethylurea (TMU) and dimethylsulfoxide (DMSO) exchanges on the tetrahedral BeS_4^{2+} in deuterated nitromethane at constant temperature. The signal at high field is due to free solvent and the other at low field to the four solvent molecules coordinated to Be^{2+}. In the DMSO case, with increasing pressures, the signals coalesce, meaning that the exchange becomes faster. The acceleration of the exchange process with pressure can be related to a bond making controlled process, whereas for TMU the reverse sequence of spectra shows a bond breaking process. Notice that the accuracy in the rate constant measurements will obviously be greater if the free and coordinated signals have similar intensity. This explains why most of the NMR relaxation rate constants for diamagnetic ions are determined in an inert diluent.

In water, though, it is much more difficult to find a suitable inert diluent, and it was thought easier to use ^{17}O line-broadening NMR in presence of Mn^{2+} (notice that ^1H cannot be used, the rate of proton exchange being usually faster than the rate of exchange of a whole water molecule). If chemical exchange is slow, the ^{17}O-NMR spectrum of a dilute aqueous solution containing an aquated metal ion consists of two resonances : a large, intense peak due to bulk H_2O, and a smaller peak due to the $M(H_2O)_n^{2+}$ resonance. A natural-abundance ^{17}O spectrum of acidified $Be(ClO_4)_2$ consists of a narrow, intense signal due to bulk H_2O at 0 ppm, and a quadruplet due to ClO_4^- at +288 ppm (Fig. 3, top). The bound-H_2O signal (dash-

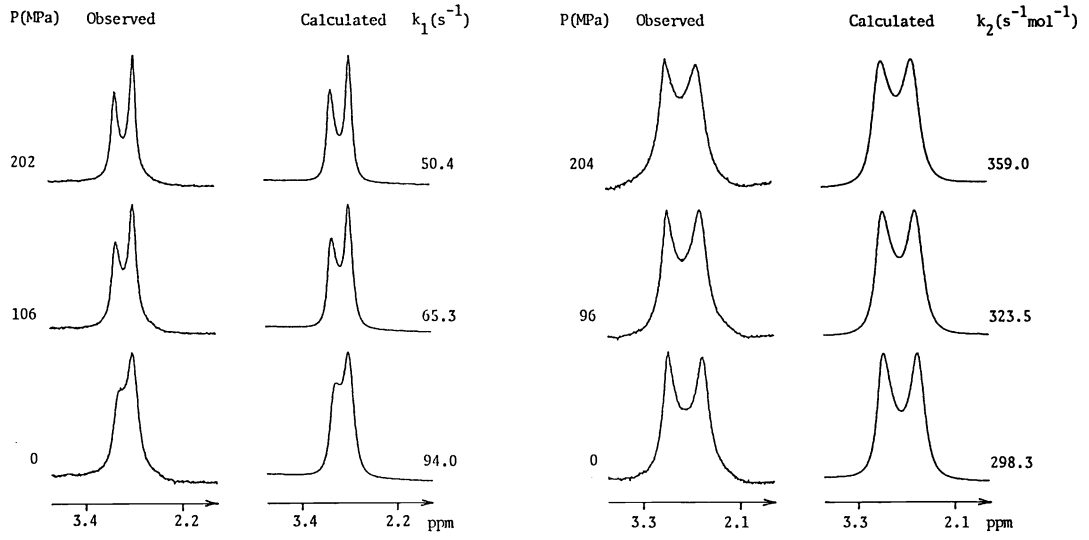

Fig. 2. Experimental and calculated 200 MHz ^{1}H-NMR spectra for TMU (left) and DMSO (right) exchanges on Be^{2+} at different pressures.

ed line), hidden under the large bulk water peak is invisible on this spectrum. The added Mn^{2+} ion is a very efficient relaxation agent for the bulk-H_2O signal due to its long electron relaxation time and its very fast coordinated/bulk H_2O exchange rate. Its addition results in an extremely broad bulk water peak with negligible amplitude, revealing the underlying kinetically interesting bound water signal (Fig. 3, bottom). It is clear from Fig. 4 that the bound-H_2O transverse relaxation rate, $1/T_2^b$ (= π x full width at half height), is dominated by quadrupolar relaxation, $1/T_{2Q}^b$, at low temperatures and by solvent exchange, k_{ex}, at high temperatures.

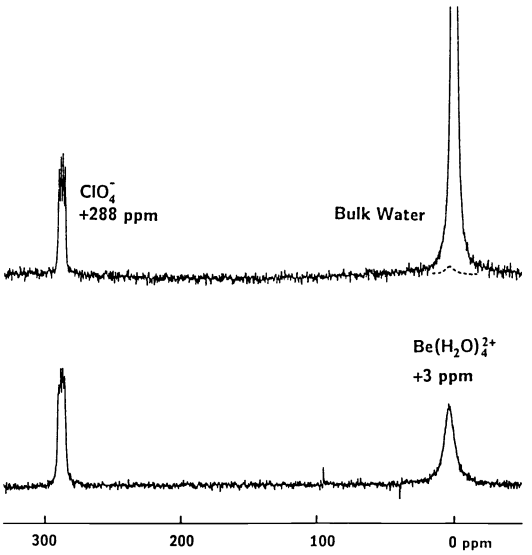

Fig. 3. 54.24 MHz ^{17}O-NMR spectra of 0.10 m $Be(ClO_4)_2$ and 0.40 m $HClO_4$ solutions, at 298 K. Top : in normal water (0.037 % ^{17}O). Bottom : in enriched water (0.40 % ^{17}O).

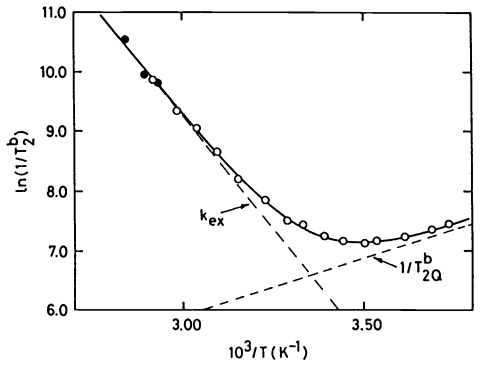

Fig. 4. Temperature dependence of the relaxation rates, $1/T_2^b$, of the bound-H_2O ^{17}O-NMR signal of 0.10 m $Be(H_2O)_4^{2+}$ solutions with added $Mn(ClO_4)_2$ and various $HClO_4$ concentrations (0.10-0.38 m), measured at 54.24 MHz.

TABLE 1. Comparison of kinetic results for the exchange of acetonitrile on $[Ni(CH_3CN)]_6^{2+}$ (ref 6.).

Year	$10^{-3}k_{298}$, s^{-1}	$\Delta H^{\#}$, kJ mol^{-1}	$\Delta S^{\#}$, $JK^{-1}mol^{-1}$	Nucleus
1967	2.8	49	-15	^{1}H
1967	3.9	46	-37	^{1}H
1967	2.1	49	-16	^{1}H
1971	2.9	67	+43	^{1}H
1971	3.0	63.2	+41.8	^{14}N
1973	2.0	68	+50	^{14}N
1973	3.6	60	+23	^{1}H
1973	14.5	39.5	-32.6	^{14}N
1978	2.9	64.6	+37.9	^{1}H

TABLE 2. Rate constants and activation parameters for solvent S exchanges on BeS_4^{2+} (from ref. 12).[a]

Solvent	k_{ex}^{298}	$\Delta H^{\#}$ kJ mol^{-1}	$\Delta S^{\#}$ JK^{-1}mol^{-1}	$\Delta V^{\#}$ cm^3 mol^{-1}	Mech.
H_2O	730[b,d]	59.2	+8.4	-13.6 (321-330 K)[f]	A
DMSO	213[c]	35.0	-83.0	-2.5 (300 K)[f]	A, I_a
TMP	4.2[c]	43.5	-87.1	-4.1 (371 K)[f]	A, I_a
DMF[e]	16[c]	52.0	-47.5	-3.1 (326 K)[f]	A, I_a
	0.2[b]	74.9	-7.3	-	D
TMU	1.0[b]	79.6	+22.3	+10.5 (346 K)[g]	D
DMPU	0.1[b]	92.6	+47.5	+10.3 (358 K)[g]	D

[a]In CD_3NO_2 as diluent by ^{1}H-NMR, except for H_2O in neat water by ^{17}O-NMR. [b]First order rate constant (s^{-1}). [c]Second order rate constant (m^{-1} s^{-1}). [d]Rate constant and $\Delta S^{\#}$ for exchange of a particular water molecule recalculated to second order units, i.e. $k_{ex}^{298}/55$: 13.1 m^{-1} s^{-1} and -24.9 JK^{-1} mol^{-1}. [e]Two terms rate law. [f]Linear fit of $\Delta V^{\#}$. [g]Quadratic fit of $\Delta V^{\#}$, 10^2 x $\Delta\beta^{\#}$ (cm^3 mol^{-1} MPa^{-1}) = +2.0(TMU) and +2.4(DMPU).

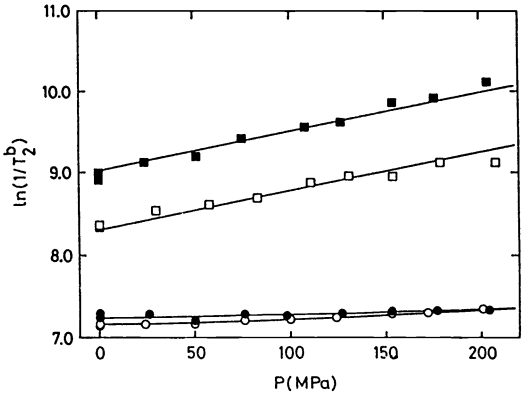

Fig. 5. Pressure dependence of $1/T_2^b$ in an acidified 0.10 m $Be(H_2O)_4^{2+}$ solution with added $Mn(ClO_4)_2$ in the exchange (■: 330 K, □: 321 K) and the quadrupolar (●: 274 K, ○: 278 K) regions, measured at 27.11 MHz.

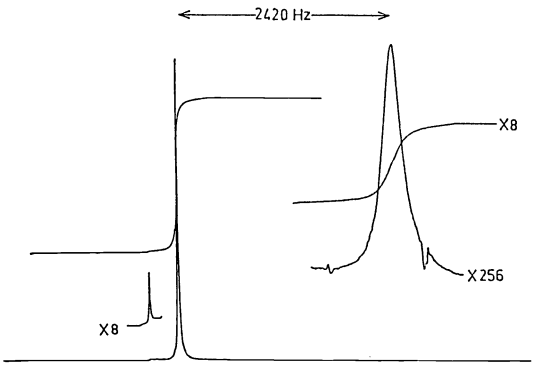

Fig. 6. 60 MHz ^{1}H-NMR spectrum of 0.1 m $Ni(MeCN)_6^{2+}$ in MeCN at 251 K with signal integrals. The resonances are (left to right) : 1 % internal benzene reference, free solvent and bound solvent.

A double exponential analysis of the data according to Eqn. 4 leads to the temperature activation parameters for both processes (see Table 2). Experiments performed at high temperature (Fig. 5) show a broadening of the bound-H_2O signal when the pressure is increased, indicative of a bond-making process for water exchange on $Be(H_2O)_4^{2+}$.

$$1/T_2^b = k_{ex} + 1/T_{2Q}^b = k_BT/h \exp(\Delta S^{\#}/R - \Delta H^{\#}/RT) + (1/T_{2Q}^b)^{298} \exp[E_Q^b/R(1/T - 1/298.2)] \quad (4)$$

For paramagnetic ions, the situation is different as shown in Fig. 6 for a dilute solution of Ni^{2+} in neat acetonitrile (ref. 6). At low temperatures, the large sharp signal corresponds to free solvent, and the very small broad peak to the resonance of the six bound acetonitrile molecules, broadened by the paramagnetic influence of the proximate Ni^{2+} center. As the temperature increases, the peaks broaden and move together, eventually coalescing into a single broad peak. The reduced linewidth $1/T_{2r}$ of the free solvent is related to the rate constant $k_{ex} = 1/\tau_m$ and to the NMR parameters T_{2m}, T_{2os} and $\Delta\omega_m$ through a complex equation (Eqn. 5) proposed by Swift and Connick (ref. 5). All show a marked tem-

$$\frac{1}{T_{2r}} = \frac{1}{\tau_m}\left[\frac{T_{2m}^{-2} + (T_{2m}\,\tau_m)^{-1} + \Delta\omega_m^2}{(T_{2m}^{-1} + \tau_m^{-1})^2 + \Delta\omega_m^2}\right] + \frac{1}{T_{2os}} \quad (5)$$

perature (and pressure to some extent) dependence which complicates the extraction of rate data. This function, illustrated in Fig. 7, can be separated into four regions characterized by different predominant relaxation processes. The region where $\ln(1/T_{2r})$ is roughly

proportional to the exchange rate ($1/\tau_m$) is called the slow exchange domain. The temperatures corresponding to this region are ideal for the study of the effect of pressure on the rate constants with small or negligible contributions from the other relaxation processes. For Ni^{2+}, the line-narrowing observed corresponds to a decrease in the exchange rate (Fig. 8) reflected by a $\Delta V^{\#}$ value of +9.6 $cm^3\ mol^{-1}$. It should be stressed that the sign of $\Delta V^{\#}$ is given unambiguously by the data. The experimental errors on $\Delta V^{\#}$ are of the order of ± 1 $cm^3\ mol^{-1}$ or ± 10 %, whatever the greatest, under normal experimental conditions. This is not the case for $\Delta S^{\#}$, obtained by extrapolation of the Eyring plot at 1/T=0, which may lead to large discrepancies for paramagnetic systems as illustrated in Table 1.

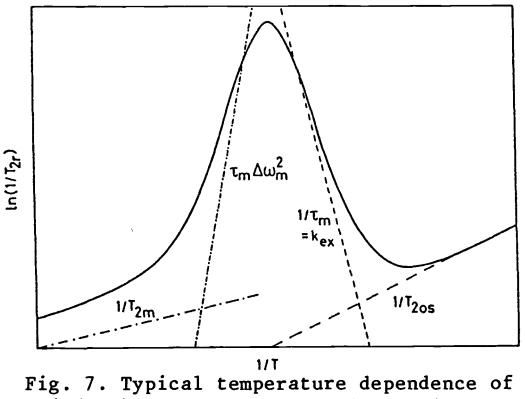

Fig. 7. Typical temperature dependence of $\ln(1/T_{2r})$. The solid curve is obtained using Eqn. 5, and the dashed lines represent the four regions where predominant relaxation contributions lead to simplification of this equation.

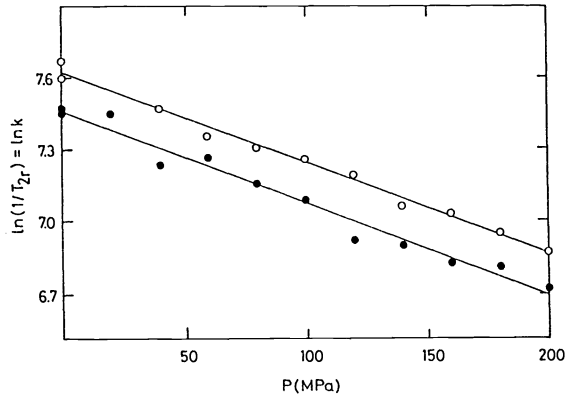

Fig. 8. Deceleration of the exchange rate with increasing pressure for MeCN exchange on $Ni(MeCN)_6^{2+}$ at two temperatures in the slow exchange domain.

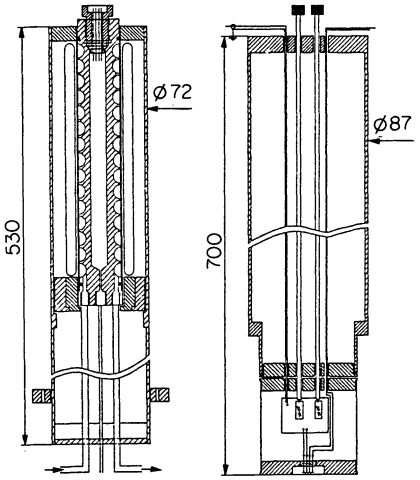

Fig. 9. Schematic drawing of the wide bore superconducting magnet multinuclear high pressure probe.

Although $\Delta S^{\#}$ values usually mimic the trends in $\Delta V^{\#}$, it has often been stressed that the large uncertainties associated with its determination by NMR line-broadening, especially in paramagnetic systems, are such as to restrict confidence in the use of this parameter to draw mechanistic conclusions.

HIGH PRESSURE HIGH RESOLUTION MULTINUCLEAR MAGNETIC RESONANCE

In 1954 already, Purcell (ref. 7), one of the founders of NMR spectroscopy, performed the first high pressure wide-line experiments on solids. In 1976 the first high pressure Fourier transform NMR probe with the high spectral resolution required to perform kinetic studies was built in our laboratory. Fig. 9 is a schematic drawing of a probe-head recently designed for wide-bore (87 mm diameter) superconducting magnets (used up to 9.4 Tesla) (ref 8). It is made of two aluminium supports. The lower one, on the left, contains the pressure bomb itself, which can be used up to 250 MPa and is made of a non-magnetic beryllium-copper alloy. Three fluid connectors are located at the bottom : one for the pressure transmitting liquid, and two for the inlet and outlet of the thermostating liquid. The upper one, with the frequency adapter box at the bottom, is shown on the right. The adapter box contains a capacitive tuning network specific for each frequency range and which must therefore be changed to observe different nuclei or to work at different magnetic fields.

This support contains two screwdrivers for access to the trimmer capacitors in the tuning network; it supports the radiofrequency connector to the spectrometer transmitter and receiver, and a platinum resistance connector to an ohm-meter for temperature measurements. The internal components of the bomb and the sample tube are shown in Fig. 10. The radiofrequency coil is wound in saddle shape on a 7 mm o.d. glass tubing to produce a radiofrequency field perpendicular to the vertical static magnetic field. The temperature is measured

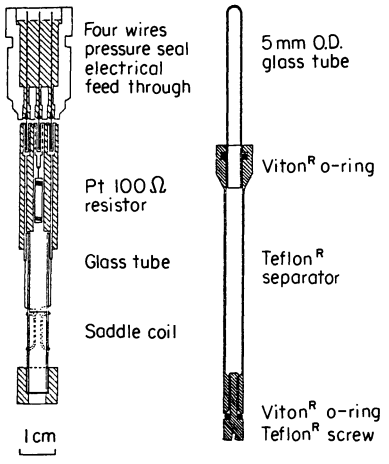

Fig. 10. Pressure seal and internal components of the bomb (left) ; sample tube and separator assembly (right).

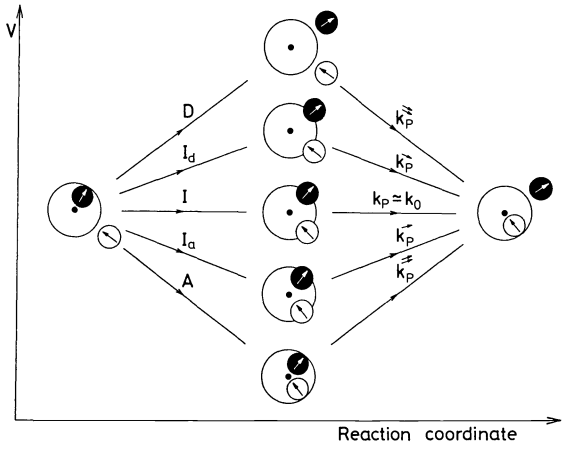

Fig. 11. Schematic representation of the transition state at crucial points in the spectrum of solvent exchange mechanisms.

inside the bomb by a platinum resistor placed just above the sample tube. The temperature stability is excellent (± 0.1 °C) and is not a limiting factor in the accuracy of measurement of $\Delta V^{\#}$. The glass tube containing the sample is a commercial 5 mm o.d. NMR tube cut to the right length. A Teflon separator transmits the hydrostatic pressure to the sample and avoids contact between the sample and the surrounding liquid. The surrounding pressure transmitting liquid is chosen as not to contain the observed nucleus. The spectral resolution and magnetic field stability observed with this non-spinning high pressure probe is as good as 1 Hz at 200 MHz, owing to the excellent homogeneity of todays superconducting magnets.

MECHANISMS

The classification of substitution reaction mechanisms originally proposed by Langford and Gray (ref. 9), and widely used in coordination chemistry, is based on operational criteria. If kinetic tests show the presence of an intermediate of increased coordination number, the mechanism is termed associative and labelled A (Fig. 11). If an intermediate of reduced coordination number can be detected, the mechanism is called dissociative and labelled D. When no intermediate species can be found, the mechanism is declared a concerted interchange process, denoted I. Within this last category, a further distinction is made, depending on whether evidence can be found for important incoming group influences (I_a) or not (I_d). As discussed by Swaddle, (ref. 10) this last operational definition is too restrictive, and so it is useful to extend it. For solvent exchange, where very few, if any, kinetic tests are applicable, this extension is critical, and opens up to the use of activation parameters as mechanistic criteria. In this context, volumes of activation are of primary importance. In a solvent exchange reaction, the electrostriction can be assumed constant throughout the reaction, and the measured volume of activation is solely constituted of the intrinsic contribution $\Delta V^{\#}_{intr}$. In this fortunate case, the sign of $\Delta V^{\#}$ therefore gives an immediate diagnostic of the activation mode. The symmetrical nature of this exchange offers other simplifications. Microscopic reversibility imposes that the forward reaction path be symmetrical to the reverse one. Hence, for limiting A or D mechanisms, with a reactive intermediate, the two transition states present along the reaction coordinate must necessarily have identical energies. Along the same line, in an interchange process, with no true energy minimum in the reaction coordinate, the bond lengths to the entering and leaving solvent molecules must be equivalent. It follows that for an I_a mechanism, the incoming and outgoing entities will both have the same and considerable bonding at the transition state, whereas for an I_d mechanism, both bonds will be as weak. From a structural point of view, the only difference between the two mechanisms resides in the degree of expansion or contraction of the transition state. If the bond distances between the central ion and the non-exchanging ligands remain unaltered during the activation step, the volume of activation is a direct measure of the degree of associativity or dissociativity of the exchange reaction considered. A continuous spectrum of transition state configurations can be envisaged, ranging from a very compact, highly associative one, with a large negative $\Delta V^{\#}$ value, to a very expanded, highly dissociative one with a large positive $\Delta V^{\#}$ value. At each extremity of this spectrum, limiting activation volumes $|\Delta V^{\#}_{lim}|$ will be found for A and D mechanisms. For interchange mechanisms characterized by $\Delta V^{\#}$ equal to zero or very small, the activation mode cannot be specified, and no subscript is associated to I.

There has been considerable enthusiasm in recent years in collecting variable pressure data on solvent exchange kinetics, acknowledging in this way that the volume of activation is almost the only criterion to get a better understanding of their mechanisms.

SOLVENT EXCHANGE ON TETRAHEDRAL SOLVATES OF Be^{2+}

Lincoln and coworkers (ref. 11) have studied a series of non-aqueous solvent exchange reactions on the small tetrahedrally coordinated Be^{2+} ion in the diluent nitromethane. They have shown that the steric character of the solvent is an important factor determining the solvent exchange mechanism on that ion. We have complemented their work by a study as a function of pressure (Table 2). For the bulkier solvents tetramethylurea (TMU) and dimethylpropyleneurea (DMPU), the rate law is first order, and the $\Delta S^{\#}$ and $\Delta V^{\#}$ are clearly positive. The conjunction of these facts indicates the occurrence of a limiting dissociative D mechanism, whereas for trimethylphosphate (TMP) and dimethylsulfoxide (DMSO) the second order rate law and the negative $\Delta S^{\#}$ and $\Delta V^{\#}$ suggest an associative activation mode for solvent exchange. The small absolute value for $\Delta V^{\#}$ does not allow the distinction between an associative interchange I_a and a limiting associative A mechanism. In the latter case, one may well imagine a large negative value due to bond formation, partially compensated by a positive contribution due to bond lengthening of the non-exchanging solvent molecules in a sterically crowded five coordinate intermediate. For DMF, both dissociative and associative pathways compete as indicated by the two terms rate law.

Our study of water exchange on Be^{2+}, performed in neat solvent, shows no acid dependence between 0.1 and 0.4 m $HClO_4$. The variable temperature data yield a value of $\Delta S^{\#}$ close to zero, therefore mechanistically useless. On the other hand, the $\Delta V^{\#}$ value of -13.6 cm^3 mol^{-1}, the most negative ever obtained for water exchange at a metal ion, is clearly indicating an associative activation mode. The partial molar volume of a water molecule electrostricted in the second coordination sphere can be estimated of about -15 cm^3 mol^{-1} (ref. 13). The measured $\Delta V^{\#}$ approaches this value which can reasonably be estimated as a maximum for an A mechanism, assuming that the incoming water molecule is accomodated into an intermediate without any increase in volume accompanying the conversion of the tetrahedral initial state into a pentacoordinated intermediate. The assignment of an A mechanism for the small water molecule confirms that a sterically governed mechanistic changeover is taking place for solvent exchange on the small Be^{2+} ion.

SOLVENT EXCHANGE ON OCTAHEDRAL METAL IONS

Trivalent cations

Solvent exchange around some diamagnetic trivalent metal ions has been studied by NMR (Table 3). In non-aqueous solvents, the studies are performed in the inert diluent, nitromethane, permitting the determination of the rate law. In the case of $Sc(TMP)_6^{3+}$, the similarity of the results obtained for TMP exchange in neat solvent and in nitromethane gives confidence that this diluent does not significantly affect the reaction mechanism. The results for Al^{3+} and Ga^{3+} are very convincingly conclusive of a dissociative activation mode, supported by the first order rate laws and the large positive entropies and volumes of activation. For Sc^{3+} and In^{3+}, they are as convincing of an associative activation mode, in view of the second order rate laws and the negative sign of the entropies and volumes of activation. The water-exchange results obtained in neat solvent are very welcome, since earlier ambient pressure results (ref. 14) suggested an associative behaviour for Ga^{3+} substitution in non-aqueous solutions. The mechanistic picture now seems more consistent in all solvents studied. The smaller Al^{3+} and Ga^{3+} cations, being rather crowded, are easily

TABLE 3. Kinetic parameters for solvent exchange on diamagnetic trivalent cations in CD_3NO_2 as diluent.

	r_i pm	k_1^{298} s^{-1}	k_2^{298} s^{-1} mol^{-1}	$\Delta H^{\#}$ kJ mol^{-1}	$\Delta S^{\#}$ JK^{-1} mol^{-1}	$\Delta V^{\#}$ cm^3 mol^{-1}	Mech.	Ref.
$Al(H_2O)_6^{3+}$[a]	54	1.29		84.7	+41.6	+5.7	I_d	15
$Al(DMSO)_6^{3+}$		0.30		82.6	+22.3	+15.6	D	16
$Al(DMF)_6^{3+}$		$5x10^{-2}$		88.3	+28.4	+13.7	D	16
$Al(TMP)_6^{3+}$		0.78		85.1	+38.2	+22.5	D	17
$Ga(H_2O)_6^{3+}$[a]	62	$4.0x10^2$		67.1	+30.1	+5.0	I_d	18
$Ga(DMSO)_6^{3+}$		1.87		72.5	+3.5	+13.1	D	16
$Ga(DMF)_6^{3+}$		1.72		85.1	+45.1	+7.9	D	16
$Ga(TMP)_6^{3+}$		6.4		76.5	+27.0	+20.7	D	17
$Sc(TMP)_6^{3+}$[a]	75	736	85	34.1	-75.6	-23.8	A,I_a	17
$Sc(TMP)_6^{3+}$			39	21.2	-143.5	-18.7		17
$In(TMP)_6^{3+}$	80		7.6	32.8	-118	-21.4	A,I_a	17

[a]In neat solvent.

willing to expel a solvent molecule from their first coordination sphere at the transition state, whereas Sc^{3+} and In^{3+}, much larger, will more readily host a seventh molecule around them, at least partially, in forming the activated complex.

A more difficult task nonetheless remains, which is to distinguish between interchange and limiting mechanisms. For water exchange on octahedral first row transition metal ions, Swaddle used a semi-empirical approach to predict average $|\Delta V^{\#}_{lim}|$ values of 13.5 cm^3 mol^{-1} for trivalent ions and 13.1 cm^3 mol^{-1} for divalent ions, almost independent of the limiting mechanism (A or D) envisaged. For water exchange on Al^{3+} and Ga^{3+}, the volumes of activation are well below the proposed limit and below the highest positive value so far obtained on an hexaaqua metal ion, +7.9 cm^3 mol^{-1} for Ni^{2+} : these reactions can therefore be considered to proceed via dissociative interchanges (I_d). In non-aqueous solvents, assignment of a D mechanism can be proposed for both ions on the basis of the first-order rate laws which could be revealed and is consistent with the larger activation volumes. For Sc^{3+} and In^{3+}, it is more difficult to decide whether A or I_a mechanisms are operative, since both are compatible with observed second order rate laws. Nevertheless, the similarity of the $\Delta V^{\#}$ values with the volume of reaction for addition of TMP on $Nd(TMP)_6^{3+}$ (r_i = 98 pm), $\Delta\bar{V}$ = -23.8 cm^3 mol^{-1} (ref. 19), suggests a common A mechanism for both ions.

These data illustrate the relationship between the increasing size of central ions and the mechanism : dissociative, associative and finally even a solvation equilibrium between a six- and a seven-coordinate solvated ion.

TABLE 4. Volumes of activation for solvent S exchange on MS_6^{3+} of the first row transition metal series (from ref. 1).[a]

M^{3+}	Sc	Ti	V	Cr	Fe	Ga
r_i(pm)	75	67	64	61	64	62
e_d^-	t_{2g}^0	t_{2g}^1	t_{2g}^2	t_{2g}^3	$t_{2g}^3e_g^2$	$t_{2g}^6e_g^4$
S=						
H_2O		-12.1	-8.9	-9.6	-5.4	+5.0
DMSO				-11.3	-3.1	+13.1[b]
DMF				-6.3	-0.9	+7.9[b]
TMP	-21.3					+20.7[b]

[a]By NMR except for Cr^{3+} by isotopic labelling. [b]In CD_3NO_2 as diluent.

A general view of the volumes of activation for first row high spin transition metal ions is given in Table 4. A definite trend is observable across the series. The $\Delta V^{\#}$ values are decreasingly negative on going along to Fe^{3+}, with a positive value for Ga^{3+}. This change-over in mechanism from associative to dissociative activation mode is confirmed by the few results in non-aqueous solvents. The value for Ti^{3+} is markedly more negative than those for the following three members of the series. It is also rather close to the limiting value of -13.5 cm^3 mol^{-1} yielded by the semi-empirical model of Swaddle. Therefore, although a limiting associative mechanism cannot be attributed on the sole basis of this value, the character of water exchange on this center can be asserted to be strongly associative. The smaller value for V^{3+}, Cr^{3+} and especially Fe^{3+} tend, on the other hand, to favor the conclusion that an associative interchange (I_a) is occurring for these three cations.

TABLE 5. Rate constants and activation parameters for water exchange on some hexaaqua and monohydroxypentaaqua metal ions.

	k^{298}[a]	k_{OH}/k_{ex}	$\Delta H^{\#}$ kJ mol^{-1}	$\Delta S^{\#}$ $JK^{-1}mol^{-1}$	$\Delta V^{\#}$ cm^3 mol^{-1}	pK_a	Ref.
Ga^{3+}	4.0×10^2 s^{-1}	275	67.1	+30.1	+5.0	~3.9	18
$Ga(OH)^{2+}$	1.4×10^1 m s^{-1}		110.9	+149.2	+7.7		
	1.1×10^5 s^{-1}		58.9	-	+6.2		
Fe^{3+}	1.6×10^2 s^{-1}	750	64.0	+12.1	-5.4	2.9	20
$Fe(OH)^{2+}$	1.5×10^2 m s^{-1}		-	-	+7.8		
	1.2×10^5 s^{-1}		42.4	+5.3	+7.0		
Cr^{3+}	2.4×10^{-6} s^{-1}	75	108.6	+11.6	-9.6	4.1	21
$Cr(OH)^{2+}$	1.4×10^{-8} m s^{-1}		148.9	+10.7	-1.1		
	1.8×10^{-4} s^{-1}		110.0	+55.6	+2.7		
Ru^{3+}	3.5×10^{-6} s^{-1}	170	89.8	-48.2	-8.3	2.7	22
$Ru(OH)^{2+}$	1.1×10^{-6} m s^{-1}		136.9	+100.5	-2.1		
	5.9×10^{-4} s^{-1}		95.8	+14.9	+0.9		

[a]In order k_{ex}, $k_{OH} \times K_a$, k_{OH}.

For Ga^{3+}, Fe^{3+}, Cr^{3+} and the low spin Ru^{3+} in water, hydrolysis is kinetically important. The conjugated base is in equilibrium with the hexaaquaion (Eqn. 6), offering an alterna-

$$M(H_2O)_6^{3+} \underset{}{\overset{K_a}{\rightleftharpoons}} M(H_2O)_5OH^{2+} + H^+ \qquad (6)$$

tive pathway for water exchange, which must be accounted for. The overall observed rate constant will therefore be the sum of contributions from the two reaction paths, the water exchange on the hexaaqua species with rate constant k_{ex} and on its hydrolysed form with rate constant k_{OH} (Eqn. 7). Two main features are apparent from the rate constants and

$$k = k_{ex} + k_{OH} \cdot K_a/[H^+] \qquad (7)$$

activation parameters reported in Table 5 : a higher reactivity (by a factor 75 to 750) and a larger dissociative character (more positive activation volumes) for the water exchange on the monohydroxypentaaqua metal ions. This drastic mechanistic difference between both exchange paths may be due to the strong electron donating capability of HO^-. The strong bonding between the metal center and this group will weaken the remaining metal-water bonds, most probably the trans one. The complex thus becomes more labile and dissociative activation is favoured.

Divalent cations

Some information from variable pressure data is available on almost every octahedral divalent member of the first row transition metal series, as apparent from Table 6. Ni^{2+} and Co^{2+} were the first cations studied, and the relatively large positive volumes of activation encountered, both in water and non aqueous solutions, supported the idea of a dissociative interchange mechanism operative for reactions involving the ions of this series.

TABLE 6. Volumes of activation for solvent S exchange on MS_6^{2+} of the first row transition metal series by NMR (from ref. 1)

M^{2+}	V	Mn	Fe	Co	Ni	Cu
r_i(pm)	79	83	78	74	69	(73)[a]
e_d^-	t_{2g}^3	$t_{2g}^3 e_g^2$	$t_{2g}^4 e_g^2$	$t_{2g}^5 e_g^2$	$t_{2g}^6 e_g^2$	$(t_{2g}^6 e_g^3)$
S						
H_2O	-4.1	-5.4	+3.8	+6.1	+7.2	
MeOH		-5.0	+0.4	+8.9	+11.4	+8.3
MeCN		-7.0	+3.0	+8.1	+8.5	
DMF			+8.5	+6.7	+9.1	
NH_3[b]					+5.9	

[a]Effective ionic radius. [b]In 15 M aqueous NH_3.

This idea proposed by Eigen and Wilkins in the sixties, (ref. 23, 24) was grounded on a comparison of ultrasonic absorption data of aqueous metal sulfates (ref. 25) with water exchange rates on the same series, Mn^{2+}, Fe^{2+}, Co^{2+} and Ni^{2+} (ref. 5). The ultrasonic relaxation spectra could be separated into the first fast formation of an outer-sphere encounter complex, followed by the rate-determining slow interchange of a water molecule for a sulfate ligand in the first hydration sphere, as shown in Eqn. 8, neglecting charges. The close

$$M(H_2O)_6 + L \underset{}{\overset{K_{os}}{\rightleftharpoons}} M(H_2O)_6 \cdots L \xrightarrow{k_I} M(H_2O)_5L + H_2O \qquad (8)$$

similarity between the rate of interchange in Eqn. 8 and the water exchange rate for a given cation led Eigen and Wilkins, although the latter author slightly revised his views for Mn^{2+} later on (ref. 26), to conclude that k_I was independent of the nature of the entering ligand, and hence, that a dissociative interchange was the rule throughout the series. The variable pressure NMR results obtained subsequently for V^{2+}, Mn^{2+}, and even Fe^{2+}, forced though to depart from this, at the time commonly accepted, concept (ref. 27). It is now generally accepted that a gradual changeover is occurring across the series, from the associatively activated V^{2+} to the dissociatively activated Ni^{2+}, at least in water, methanol and acetonitrile (Table 6). The small $\Delta V^{\#}$ values for Fe^{2+} are indicative of an interchange mechanism with almost as much contribution from bond making as from bond breaking. Considering the mean limiting values of $|\Delta V^{\#}_{lim}| = 13.1$ cm^3 mol^{-1} obtained from Swaddle's model in the extreme cases of A and D mechanisms for water exchange on divalent cations, one is tempted to attribute interchange mechanisms to every cation in Table 6, in view of the lower values of the volumes of activation reported. This assignment is also supported by zero or very small values of $\Delta\beta^{\#}$ in neat solvent (ref. 17). In water, methanol and acetonitrile, the changeover can therefore be assumed to proceed from an associative interchange for the early members of the series to a dissociative interchange for the late mem-

TABLE 7. Volumes of activation, $\Delta V_I^{\#}$,[a] for the interchange of neutral and uninegative ligands on M^{2+} ions in water.

Ligand	V^{2+}	Mn^{2+}	Fe^{2+}	Co^{2+}	Ni^{2+}	Cu^{2+}	Zn^{2+}	Ref.
H_2O	-4.1	-5.4	+3.8	+6.1	+7.2			28,29
NH_3				+4.8	+6.0			30
imidazole					+11.0			31
isoquinoline					+7.4			32
PADA[b]				+7.9[e]	+7.1[e]			30,33,34
bipy[c]		-1.2		+5.9[e]	+5.3[e]			35,36
terpy[d]		-3.4	+3.6	+4.1	+5.6			37,36
SCN^-	-5.3							38
glycinate (1-)				+5	+7	+9	+4	39
murexide (1-)					+8.7			40

[a] in $cm^3\ mol^{-1}$; $\Delta V_I^{\#} = \Delta V_f^{\#} - \Delta V_{os}^{0}$; $\Delta V_{os}^{0} = 0$ for neutral ligands, $\Delta V_{os}^{0} = +3.2\ cm^3\ mol^{-1}$ for uninegative ligands, [b] pyridine-2-azo-(p-dimethylaniline), [c] 2,2'-bipyridine, [d] 2,6-bis(2'-pyridyl)pyridine, [e] average value.

bers, with the change in activation mode from the d^5 to the d^6 configuration. The situation is much less clear in DMF. The value of $\Delta V^{\#} = +8.5\ cm^3\ mol^{-1}$ recently obtained for Fe^{2+} tends to suggest that bond breaking is more important in this bulky solvent than in the other three. Steric effects in DMF were already noticed for solvent exchange on the tetrahedral Be^{2+} ion (Table 2). In this context, the volume of activation for DMF exchange on Mn^{2+} is looked forward to with impatience.

In water, a few complex formation reactions involving the early elements of the series have been studied as a function of pressure so far, the largest number being centered on Ni^{2+} or Co^{2+} (Table 7). The conclusions of all these studies totally corroborate the assignments previously made on the basis of the solvent exchange data.

Synthetic view

The systematic trend observed along the first row transition metal series for the divalent as well as for the trivalent cations can be visualized, following Swaddle (ref. 2), with the aid of a two dimensional More O'Ferral type plot (Fig. 12). The sum of the coordinates of each point along a trajectory represents the change in volume to reach that point. The volume of activation is obtained at the intersection with the dashed diagonal. It should be noted, however, that this square representation imposes that the activation volumes for the two limiting mechanisms be represented by the same absolute value at the corners. In this diagram, we have chosen as limiting values for A and D mechanisms the $\Delta V^{\#}_{lim}$ yielded by Swaddle's semi-empirical treatment, which fortuitously come out as approximately equal. Looking closer at Fig. 12, though, the possibility cannot be excluded that the extreme value for a dissociative process might be less than proposed by Swaddle's model.

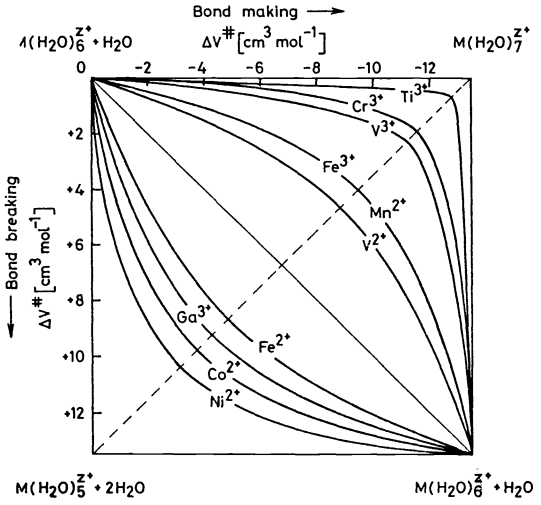

Fig. 12. Bond making and bond breaking contributions to the volumes of activation for water exchange on $M(H_2O)_6^{z+}$

The observed progressive changeover cannot be explained in terms of cationic size or charge only, as was done for the limited group of the diamagnetic trivalent ions discussed earlier. The electronic configuration in the valence shell also bears an important role in the mechanistic behaviour of these d elements. For a σ bonded octahedral complex, the t_{2g} orbitals are non-bonding whereas the e_g orbitals are anti-bonding. Certainly, the gradual filling of the t_{2g} orbitals, spread out between ligands, will electrostatically disfavour the approach of a seventh molecule towards a face of the octahedron, and therefore decrease the ease of bond making. Similarly, an increased occupancy of the e_g orbitals, pointed to the ligands, will enhance the bond breaking tendency. These effects, combined with the steric effects outlined above, can explain the sequences of $\Delta V^{\#}$ values in Tables 4 and 6, with the exception of the values reported for V^{3+} or Cr^{3+}, which remain too low or too high, respectively. But this small discrepancy is not real since the value of $\Delta V^{\#}$ cannot be determined better than within $\pm 1\ cm^3\ mol^{-1}$ as discussed before. In any case, we are unable to distinguish which effect predominates, although the smaller value reported for V^{2+} ($t_{2g}^3 e_g^0$, $r_i = 79$ pm) compared to that for Mn^{2+} ($t_{2g}^3 e_g^2$, $r_i = 83$ pm) seems to indicate that the e_g filling more than compensates the steric effect.

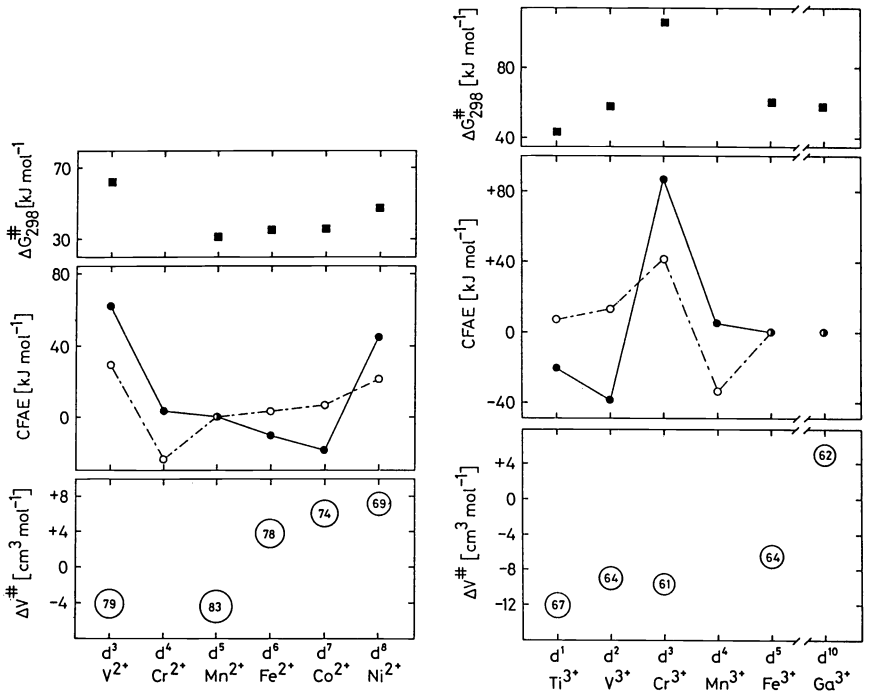

Fig. 13. Free activation energies, calculated crystal field activation energies (CFAE) (closed circles for A and open circles for D) and activation volume for water exchange on high spin $M(H_2O)_6^{2+}$ and $M(H_2O)_6^{3+}$ (ionic radii, in pm, are given in the circles).

Fig. 13 shows the sequencies in activation volumes along the divalent and trivalent series in a pictorial form. Above these, the corresponding crystal field activation energies (CFAE) are displayed. Reactivities of octahedral transition metal ions towards substitution are often correlated with crystal field stabilization. The CFAE's can be calculated for high and low spin states as the difference in stabilization between the transition state geometry (pentagonal bipyramid for A, octahedral wedge for I and square pyramid for D) and the octahedral ground state (ref. 41). As shown in Fig. 13, A or D models equally well explain the trends in lability observed in the two series. The CFAE's are therefore of no help in mechanistic prediction. The free energies of activation $\Delta G^{\#}$ nicely parallel the CFAE's, but there is of course no direct correlation between the $\Delta G^{\#}$ and the activation volumes. This does not imply that the suggested correlation between $\Delta S^{\#}$ and $\Delta V^{\#}$ (ref. 42) does not exist, but even though some form of relation between the randomness at the transition state and its degree of expansion or contraction might be expected, there is no necessary thermodynamic relationship between entropy and volume.

CONCLUSION

In 1973, Stranks (ref. 13) could present all available data in the field of high pressure inorganic reaction mechanism during his plenary lecture at the XVth International Conference on Coordination Chemistry held in Moscow. Since then this field has exploded with more than 800 references available, collected in a book edited this year by van Eldik (ref. 1). Volumes of activation are now recognized as one of the major kinetic criteria for inorganic mechanistic assignements. Most high pressure kinetic equipments are now commercially available or described in the literature and easy to build. The sign of the activation volume is unambiguously related to the acceleration or retardation of a rate constant with pressure and the $\Delta V^{\#}$ values being expressed in volume per mole can easily be visualized and modelized. However, like for other activation parameters, the usefullness of $\Delta V^{\#}$ for mechanistic discrimination is limited by the complexity of the reactions studied. I hope to have demonstrated that the high pressure approach is ideal for solvent exchange reactions, characterized by symmetrical pathways and no major solvationnal changes. For complex formation reactions, especially those preceeded by charge neutralization in the formation of an outer sphere complex, a more cautious interpretation is required. But nevertheless, the results produce a consistent picture with those of solvent exchange reactions. Finally it is not useless to stress that for any reaction with products different from reactants, that is a non symmetrical-reaction, it is imperative to have some knowledge of the volume profile before reaching a safe mechanistic assignment.

Acknowledgement

Portions of this text are taken from a review chapter on solvent exchange reactions written with Dr. Y. Ducommun for ref. 1, and I would like to thank him for his collaboration in preparing the present lecture. I wish also to express my thanks to Dr. L. Helm for his help in the supervision of the high pressure NMR experiments.

REFERENCES

1. High Pressure Inorganic Chemistry : Kinetics and Mechanisms, R. Van Eldik, Ed., (Elsevier, Amsterdam, 1986).
2. H.R. Hunt and H. Taube, J. Am. Chem. Soc., 80, 2642 (1958).
3. High Pressure Chemistry, H. Kelm, Ed., (Reidel, Dordrecht, 1978).
4. R.V. Southwood-Jones, W.L. Earl, K.E. Newman and A.E. Merbach, J. Chem. Phys., 73, 5909 (1980).
5. T.J. Swift and R.E. Connick, J. Chem. Phys., 37, 307 (1962) and 41, 2553 (1964).
6. K.E. Newman, F.K. Meyer and A.E. Merbach, J. Am. Chem. Soc., 101, 1470 (1979).
7. G.B. Benedek and E.M. Purcell, J. Chem. Phys., 22, 2208 (1954).
8. D.L. Pisaniello, L. Helm, P. Meier and A.E. Merbach, J. Am. Chem. Soc., 105, 4528 (1983).
9. C.H. Langford and H.B. Gray, Ligand Substitution Processes, Chapter 1, (W.A. Benjamin, New York, 1965).
10. T.W. Swaddle, Adv. Inorg. Bioinorg. Mechanisms, A.G. Sykes, Ed., 2, 95 (1983).
11. S.F. Lincoln and M.N. Tkaczuk, Ber. Bunsenges. Phys. Chem., 85, 433 (1981) and 86, 221 (1982).
12. G. Elbaze, P.-A. Pittet, L. Helm and A.E. Merbach, to be submitted.
13. D.R. Stranks, Pure Appl. Chem., 38, 303 (1974).
14. J. Miceli and J. Stuehr, J. Am. Chem. Soc., 90, 6967 (1968).
15. D. Hugi-Cleary, L. Helm and A.E. Merbach, Helv. Chim. Acta, 68, 545 (1985).
16. C. Ammann, P. Moore, A.E. Merbach and C.H. McAteer, Helv. Chim. Acta, 63, 268 (1980).
17. A.E. Merbach, Pure Appl. Chem., 54, 1479 (1982).
18. D. Hugi-Cleary, Ph.D. Thesis, University of Lausanne, 1984.
19. D.L. Pisaniello, P.J. Nichols, Y. Ducommun and A.E. Merbach, Helv. Chim. Acta, 65, 1025 (1982).
20. T.W. Swaddle and A.E. Merbach, Inorg. Chem., 20, 4212 (1981).
21. F.-C. Xu, H.R. Krouse and T.W. Swaddle, Inorg. Chem., 24, 267 (1985).
22. I. Rapaport, P. Bernhard, L. Helm, A. Ludi and A.E. Merbach, to be submitted.
23. M. Eigen, Z. Electrochem., 64, 115 (1960).
24. R.G. Wilkins and M. Eigen, Adv. Chem. Ser., 49, 55 (1965).
25. M. Eigen and K. Tamm, Z. Electrochem., 66, 93 (1962).
26. R.G. Wilkins, Acc. Chem. Res., 3, 408 (1970).
27. J. Burgess, Metal Ions in Solution, (Ellis Horwood, Chichester, 1978).
28. Y. Ducommun, D. Zbinden and A.E. Merbach, Helv. Chim. Acta, 65, 1385 (1982).
29. Y. Ducommun, K.E. Newman and A.E. Merbach, Inorg. Chem., 19, 3696 (1980).
30. E.F. Caldin, M.W. Grant and B.B. Hasinoff, J. Chem. Soc., Faraday Trans. I, 68, 2247 (1972).
31. A.D. Yu, M. D. Waissbluth and R.A. Grieger, Rev. Sci. Instrum., 44, 1390 (1973).
32. K. Ishihara, S. Funahashi and M. Tanaka, Inorg. Chem., 22, 2564 (1983).
33. E.F. Caldin and R.C. Greenwood, J. Chem. Soc., Faraday Trans. I, 77, 773 (1981).
34. R. Doss, R. van Eldik and H. Kelm, Rev. Sci. Instrum., 53, 1592 (1982).
35. R. Doss and R. van Eldik, Inorg. Chem., 21, 4108 (1982).
36. R. Mohr and R. van Eldik, Inorg. Chem., 24, 3396 (1985).
37. R. Mohr, L.A. Mietta, Y. Ducommun and R. van Eldik, Inorg. Chem., 24, 757 (1985).
38. P.J. Nichols, Y. Ducommun and A.E. Merbach, Inorg. Chem., 22, 3993 (1983).
39. M.W. Grant, J. Chem. Soc., Faraday Trans. I, 69, 560 (1973).
40. A. Jost, Ber. Bunsenges. Phys. Chem., 79, 850 (1975).
41. F. Basolo and R.G. Pearson, Mechanisms of Inorganic Reactions, (J. Wiley, New York, 1967).
42. M.V. Twigg, Inorg. Chim. Acta, 24, L84 (1977).